Available online at www.sciencedirect.com
SCIENCE DIRECT
Journal of Molecular Catalysis A: Chemical 235 (2005) 194–199
JOURNAL OF MOLECULAR CATALYSIS A: CHEMICAL
www.elsevier.com/locate/molcata

Visible light photodegradation of phenol on MWNT-TiO_2 composite catalysts prepared by a modified sol–gel method

Wendong Wang [a], Philippe Serp [b], Philippe Kalck [b], Joaquim Luís Faria [a,*]

[a] *Laboratório de Catálise e Materiais, Departamento de Engenharia Química, Faculdade de Engenharia da Universidade do Porto, Rua Dr. Roberto Frias s/n 4200-465 Porto, Portugal*
[b] *Laboratoire de Catalyse, Chimie Fine et Polymères, Ecole Nationale Supérieure d'Ingénieurs en Arts Chimiques Et Technologiques, 118 Route de Narbonne Toulouse Cedex 31077, France*

Received 27 December 2004; received in revised form 15 February 2005; accepted 18 February 2005
Available online 12 May 2005

Abstract

Multi-walled carbon nanotubes (MWNT) and TiO_2 composite catalysts were prepared by a modified sol–gel method. The nanoscaled composite materials were extensively characterized by TG, N_2 adsorption-desorption isotherm, XRD, SEM, EDX, TEM and UV–vis spectra. The photocatalytic degradation of phenol was performed under visible light irradiation on these catalysts. An optimum of synergetic effect on photocatalytic activity was observed for a weight ratio MWNT/TiO_2 equal to 20% with an increase in the first-order rate constant by a factor of 4.1. The synergetic effect, induced by a strong interphase interaction between MWNT and TiO_2, was discussed in terms of different roles played by MWNT in the composite catalysts.

Keywords: Photocatalysis; Phenol degradation; Titanium dioxide; MWNT; Composite catalysts

1. Introduction

Titanium dioxide has been extensively employed as photocatalytic material for solving environmental problems, especially for eliminating toxic chemicals from waste water [1,2]. TiO_2/UV system has been widely investigated in the heterogeneous photocatalytic process, during which UV irradiation upon the semiconductor can photoactivate TiO_2 generating electron/hole couples with strong redox properties [3]. The photocatalytic activitiy of TiO_2 powder greatly depends upon its microstructure and physical properties due to different preparation conditions and methods [4–11]. Additionally, it has been reported that activated carbon (AC) has some beneficial effects on the photocatalytic activities of TiO_2 [12–14].

The major drawback in the practical application under irradiation of natural solar light (where only approximately 4% of the solar radiation is effective) is the band gap energy (3.2 eV) for anatase TiO_2. Therefore, the development of photocatalysts that can be excited by visible light has received much attention. Various efforts have been attempted to extend the light absorption of the photocatalysts to the visible region. For example, TiO_2 impregnated with different transition metals shows a slight shift in the band gap transition to longer wavelengths and an extension of the absorption in the visible region, but also a significant reduction in photoactivity due to a higher recombination rate [15]. Rare earth cerium [16] and neodymium [17] ion modified TiO_2 sol can effectively photodegrade reactive brilliant red dye (X-3B) or phenol under visible light irradiation. Photodegradation of organic pollutants by using visible light has also been achieved on superficially modified TiO_2 with different dyestuff or complexes [18–22]. Photocatalysts based on TiO_2 for visible light degradation of *p*-chlorophenol (4CP) have been obtained by a sol–gel process using $Na_2[PtCl_6]$ as a dopant [23], calcination of gels prepared by a sol–gel process using various titanium alkoxide precursors [24] and pyrolysis of hydrolyzed $TiCl_4$ with nitrogen base [25].

* Corresponding author. Tel.: +351 225 081 645; fax: +351 225 081 449.
E-mail address: jlfaria@fe.up.pt (J.L. Faria).

1381-1169/$ – see front matter © 2005 Elsevier B.V. All rights reserved.
doi:10.1016/j.molcata.2005.02.027

In a recent review, attention has been called to the fact that carbon nanotubes (CNT) are attractive and competitive catalyst supports when compared to activated carbon due to the combination of their electronic, adsorption, mechanical and thermal properties [26]. The unique electronic properties of CNT are that they can be either metallic or semiconducting, depending on their geometry [27]. Composites containing CNT are believed to provide many applications and exhibit cooperative or synergetic effects between the metal oxides and carbon phases. In the case of TiO_2, several recent works have emphasized on the preparation of the new hybrid materials [28–31], but the only reported study on this matter with low CNT content (1.5 wt.%) failed to confirm this prediction in phenol degradation under UV illumination [32]. On the basis of our preliminary work that revealed a considerable synergetic effect of multi-walled carbon nanotubes (MWNT) and TiO_2 composite catalysts with higher MWNT content on phenol degradation under UV light [33], the application of these materials is here extended for the first time to visible light photodegradation of phenol.

2. Experimental

2.1. Catalysts preparation

High purity MWNT were synthesized by a catalytic chemical vapour deposition (CCVD) method in fluidised bed reactor on a Fe/Al_2O_3 catalyst, and their purification was achieved according to a standard sulphuric acid washing procedure [34]. MWNT-TiO_2 composite catalysts were prepared by a modified acid-catalyzed sol–gel method from alkoxide precursors. The preparation was performed at room temperature as following: 0.1 mol of $Ti(OC_3H_7)_4$ (Aldrich 97%) was dissolved in 200 mL of ethanol. The solution was stirred magnetically for 30 min, and then 1.56 mL of nitric acid (65 wt.%) was added. Subsequently, certain amount of MWNT was introduced into the $Ti(OC_3H_7)_4$ ethanol solution. The mixture was loosely covered and kept stirring until a homogenous MWNT-contained gel formed. The gel was aged in air for several days. Then, the xerogel was crushed into a fine powder and dried at room temperature. The powder was calcined at 400 °C in a flow of nitrogen for 2 h to obtain MWNT-TiO_2 composite catalysts. Catalysts are named as X-MWNT-TiO_2, where X (5, 10, 20 and 40) corresponds to the weight ratio of MWNT to a 100 weight basis of neat TiO_2 (e.g. 20-MWNT-TiO_2 means 20/100 (MWNT/TiO_2, w/w)).

2.2. Characterization methods

The thermal behaviors of the xerogel and composite materials were analyzed with a Mettler TA 4000 system from 25 to 800 °C at a heating rate of 10 °C/min under N_2 or air. The carbon content in the composite catalysts was also determined from weight loss in air by using the same conditions. BET surface area was measured by N_2 adsorption–desorption isotherm using an Omnisorp 100 CX apparatus. XRD study was performed with a Philips X'Pert MPD diffractometer (Cu Kα = 0.15406 nm). The composite catalysts were characterized by TEM using a Phillips CM12 operating at 120 kV and SEM using a Jeol JSM-6301F equipped with an energy-dispersive X-ray (EDX) detector. The UV–vis spectra of the powder solids were measured on a JASCO V-560 UV–vis spectrophotometer, equipped with an integrating sphere attachment (JASCO ISV-469).

2.3. Photocatalytic reaction

Photocatalytic activities were evaluated by phenol degradation in aqueous media under visible light irradiation. The experiments were carried out in a glass immersion photochemical reactor charged with 800 mL of suspension/solution. The reactor was equipped with a visible light irradiation source (a Heraeus TQ 150 medium-pressure mercury vapor lamp), which was located axially and held in a quartz immersion tube. A circulating water jacket was employed to cool the irradiation source and cancel the infrared radiation, thus preventing any heating of the suspension.

The initial phenol concentration (C_0') was 50 mg/L. The amount of suspended TiO_2 was kept at 1 g/L, with the corresponding amount of carbon being calculated accordingly for the different composite catalysts. Before turning on illumination the suspension containig phenol and photocatalyst was magnetically stirred in a dark condition for 60 min, to establish an adsorption–desorption equilibrium. Then, the suspension was irradiated with visible light (more intense lines at λ_{exc} of 366, 456 and 546 nm, the UV line at 254 nm being filtered by the Pyrex© glass jacket filled with water) at constant stirring speed. The first sample was taken out at the end of the dark adsorption period, just before the light was turned on, in order to determine the phenol concentration in solution, which was hereafter considered as the initial concentration (C_0) after dark adsorption. Samples were then withdrawn regularly from the reactor and centrifuged immediately for separation of any suspended solid. The clean transparent solution was analyzed by UV–vis spectroscopy (JASCO V-560). The full spectrum (200–800 nm) for each sample was recorded and the absorbance at characteristic band 270 nm was followed to determine the phenol concentration. Repetition tests were made to ensure the reproducibility.

3. Results and discussion

3.1. Catalyst characterization

The carbon content of the composite catalysts determined by TG is listed in Table 1. As expected, since the materials were calcined at 400 °C in a N_2 flow for 2 h, there is no appreciable degradation of the MWNT and the determined carbon content agrees very well with the calculated value from initial ratio. EDX spectra analysis of MWNT-TiO_2

Table 1
Carbon content determined by TG (C_{TG}), BET surface area (S_{BET}), average pore size distribution and TiO_2 crystal size (d_{TiO_2}) of the MWNT-TiO_2 composite catalysts compared to the base components

Catalyst	C_{TG} (wt.%)	S_{BET} (m^2/g)	Pore size diameter (nm)	d_{TiO_2} (nm)
TiO_2	–	107	3.2	8.5 ± 0.2
5-MWNT-TiO_2	4.6	114	3.2/3.7	7.9 ± 0.1
10-MWNT-TiO_2	8.8	124	3.2/3.7	7.7 ± 0.1
20-MWNT-TiO_2	16.4	139	3.2/3.7	7.4 ± 0.1
40-MWNT-TiO_2	27.1	163	3.3/3.8	6.4 ± 0.1
MWNT	–	169	3.4/20	–

composite catalysts confirms only the presence of C, O and Ti elements.

The N_2 adsorption–desorption isotherms (shown as supplementary material) for TiO_2, MWNT, and MWNT-TiO_2 composite materials can be ascribed to type IV [35], which suggests a mesoporous pore texture. The BET surface areas (Table 1) of neat TiO_2 and MWNT are 107 and 169 m^2/g, respectively, while those of composite catalysts vary from 114 to 163 m^2/g, increasing with the initial MWNT/TiO_2 ratio from 5 to 40%. It is interesting to note that the surface areas of composite catalysts are higher than those calculated in proportion to the TiO_2 and MWNT contents. It seems that MWNT introduced into TiO_2 matrix can prevent TiO_2 particles from agglomerating, thus increasing the surface area. This result is also supported by SEM observations (not shown), in which the composite catalysts with higher MWNT content feature morphologies with relatively more homogeneous embedding in TiO_2 matrix without apparent agglomeration of the TiO_2 particles.

Average pore sizes of different solids obtained from N_2 isotherm are also given in Table 1. Pores in MWNT include narrowly distributed inner hollow cavities of 3.4 nm and widely distributed aggregated pores of 20 nm formed by interaction of isolated MWNT [26]. TiO_2 presents monomodal pore size distribution centered at 3.2 nm. All the composite catalysts reveal two different pores of adjacent diameters with different distribution ratio. 3.2 nm (3.3 nm for 40-MWNT-TiO_2) with high distribution can be attributed to TiO_2, while 3.7 nm (3.8 nm for 40-MWNT-TiO_2) with low distribution, increasing with the MWNT content, to inner hollow cavities in MWNT, while the aggregated pores in MWNT of 20 nm are absent for all the composite catalysts.

XRD patterns (shown as supplementary material) reveal that only TiO_2 in anatase phase can be identified for TiO_2 and composite catalysts. The rutile and brookite phases of TiO_2 are not observed. It is worthy of notice that the characteristic peaks of MWNT can hardly been identified from all the patterns of composite catalysts. It is observed that the peaks width broaden slightly and gradually with the increase in MWNT content for the composite catalysts. TiO_2 crystallite sizes estimated from the line broadening are given in Table 1. The neat TiO_2 of 8.5 nm size is obtained, while those of composite catalysts decrease gradually from 7.9 to 6.4 nm for 5-MWNT-TiO_2 to 40-MWNT-TiO_2, which is also confirmed by TEM observations (typically presented in Fig. 1 for 20-MWNT-TiO_2).

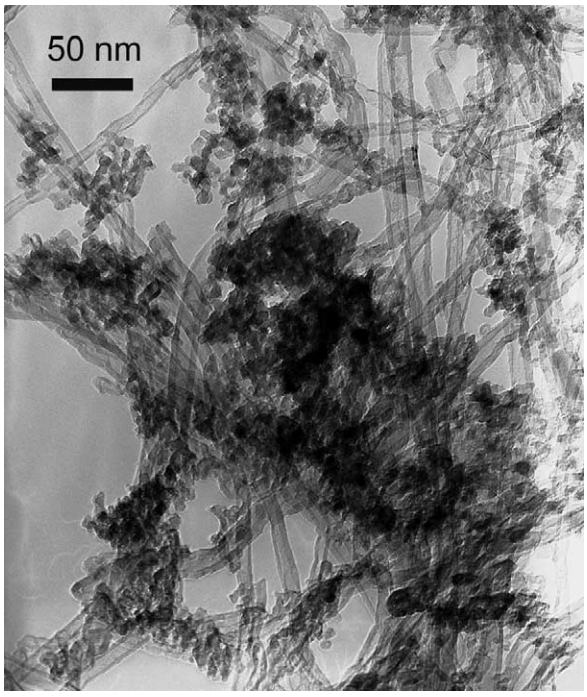

Fig. 1. TEM micrograph of the 20-MWNT-TiO_2 composite catalyst. Nanosized crystallites of TiO_2 are visible over the MWNT.

Based on the characterization mentioned above, the fact that surface areas of composite catalysts are higher than expected means that there should be a strong interphase structural effect between the carbon and metal oxide phases. The absence of MWNT aggregated pores in the composite catalysts proves a homogeneous dispersion of MWNT in TiO_2 matrix, which is also supported by the disappearance of MWNT characteristic peaks in their XRD patterns. On the other hand, higher MWNT content favors less extended crystallized TiO_2 domains on MWNT surface and thus avoiding TiO_2 particles agglomeration. Both of the factors account for the increase in surface areas of the composite catalysts.

The diffuse reflectance UV–vis spectra of the different solids expressed in terms of Kubelka-Munk equivalent absorption units are presented in Fig. 2. As expected, P25 shows the characteristic spectrum with its fundamental absorption sharp edge rising at 400 nm, while the absorption spectrum of neat TiO_2 prepared by the sol–gel method shifts a bit into visible light region. On the other hand, the composite catalysts can absorb at higher wavelengths than neat TiO_2. The absorption is even totally over the whole range of the UV–vis spectrum for 40-MWNT-TiO_2. It is noticeable that there is an obvious correlation between the MWNT content and the UV–vis spectrum change. The enhancements of absorption increase with MWNT contents of the composite catalysts. These observations might suggest an increase of surface electric charge of the oxides in the composite catalysts due to

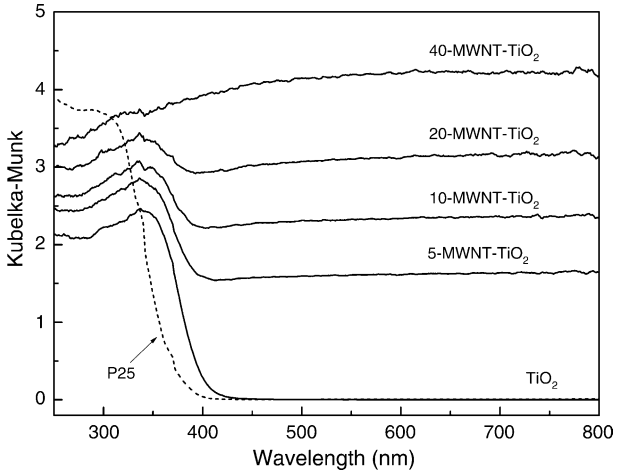

Fig. 2. Diffuse reflectance UV–vis spectra of P25, TiO_2 and MWNT-TiO_2 composite catalysts.

MWNT introduction, which may lead to modifications of the fundamental process of electron/hole pair formation while applying visible irradiation.

3.2. Photocatalytic degradation of phenol

The photodegradation of phenol in aqueous suspension containing MWNT-TiO_2 composite catalyst under visible light follows pseudo-first-order kinetics. The kinetic plots are shown by apparent first-order linear transform $\ln(C_0/C) = f(t)$ in Fig. 3.

No appreciable photodegradation can be observed in the presence of neat MWNT as well as the direct photolysis without any solid during the same irradiation time, because phenol molecule has no absorption in visible range. In the presence of P25, a negligible less than 10% conversion of phenol was observed within 3 h under the same reaction conditions, which may be due to the combination of the presence of trace UV light and an oxidation effect by dissolved oxygen in the suspension. The activity of the prepared catalysts can be evaluated by comparing the apparent first-order rate constants (k_{app}) listed in Table 2. A synergy factor (R) is defined as $R = k_{app}(\text{MWNT-TiO}_2)/k_{app}(\text{TiO}_2)$ to quantify the synergetic effect [12]. Neat TiO_2 and 20-MWNT-TiO_2 composite catalyst give apparent rate constants of $1.8 \times 10^{-3}\ \text{min}^{-1}$ and $7.4 \times 10^{-3}\ \text{min}^{-1}$, respectively. The introduction of 20% MWNT into TiO_2 matrix obviously creates a kinetic synergetic effect in phenol degradation with an increase in the rate constant by a factor of 4.1.

Table 2
Summary of visible light photodegradation of phenol on different solids at given initial concentration of phenol ($C_0' = 50$ mg/L)

Catalysts	C_0 (mg/L)	X_{5h} (%)	k_{app} ($\times 10^{-3}\ \text{min}^{-1}$)	R
TiO_2	47.5	41	1.8 ± 0.1	–
5-MWNT-TiO_2	47.2	49	2.0 ± 0.1	1.1
10-MWNT-TiO_2	46.1	63	3.2 ± 0.1	1.8
20-MWNT-TiO_2	45.4	96	7.4 ± 0.1	4.1
40-MWNT-TiO_2	44.1	86	5.4 ± 0.3	3.0
TiO_2 + 20%MWNT	46.5	71	3.3 ± 0.1	1.8

The complete disappearance of phenol (more than 95% conversion) on 20-MWNT-TiO_2 can be achieved within 5 h during a long-term running photoreaction (Fig. 4). By contrast, phenol conversions after 5h of irradiation (X_{5h}) are also compared in Table 2. Neat TiO_2 can only reach 40.6% of phenol conversion within the same reaction time, and complete elimination of phenol is expected to take place in more than 10 h.

The influence of MWNT content upon the kinetics of phenol removal is shown in Fig. 5. The synergetic effect between TiO_2 and MWNT on the photocatalytic degradation of phenol clearly exists for all the composite catalysts. An optimum of the synergetic effect is found for 20-MWNT-TiO_2 with a weight ratio MWNT/TiO_2 equal to 20%. The increase in weight ratio MWNT/TiO_2 from 5 to 20% favors the syn-

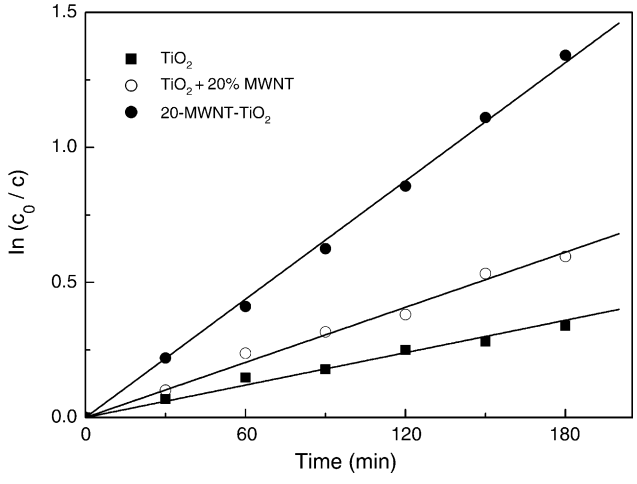

Fig. 3. Apparent first-order linear transform $\ln(C_0/C) = f(t)$ of phenol degradation kinetic plots for TiO_2, 20-MWNT-TiO_2 composite catalyst and mechanical mixture with the same MWNT content.

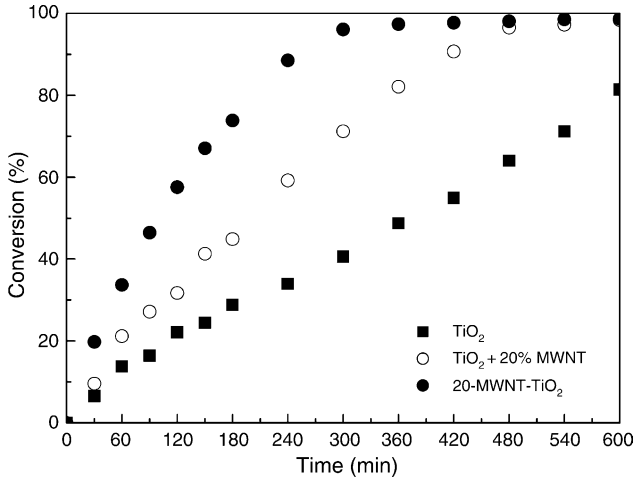

Fig. 4. Conversion of phenol photodegradation for TiO_2, 20-MWNT-TiO_2 composite catalyst and mechanical mixture with the same MWNT content.

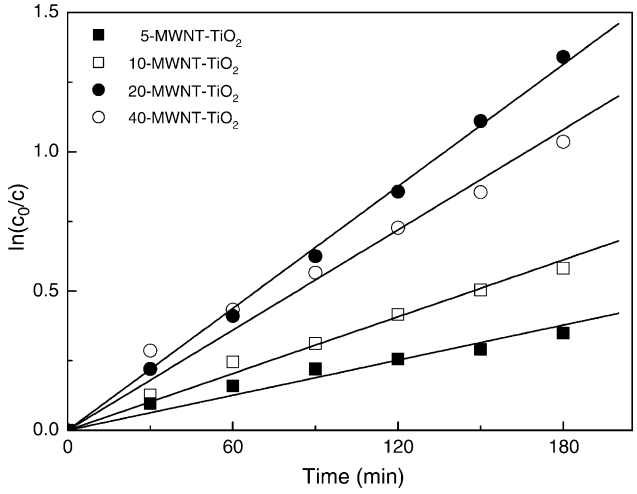

Fig. 5. Apparent first-order linear transform $\ln(C_0/C) = f(t)$ of phenol degradation kinetic plots for MWNT-TiO_2 composite catalysts with different MWNT content.

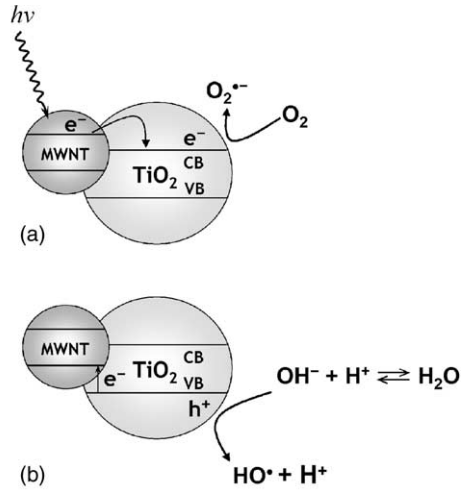

Scheme 1. MWNT acting as photosensitizer in the composite catalyst: (a) electron injection into the conduction band of TiO_2 semiconductor; (b) electron back-transfer to MWNT with the formation of a hole in the valence band of TiO_2 semiconductor and reduction of the so formed hole by adsorbed OH^- oxidation.

ergetic effect on phenol removal, indicating the increase in synergy factor from 1.1 to 4.1, which may be correlated to the UV–vis absorption spectra changes of the solids. The decrease in activity with higher MWNT/TiO_2 weight ratio is considered to be related to increasedly absorbing and scattering of photons by surplus carbon in the photoreaction system.

A suspended mechanical mixture of 20% MWNT and TiO_2 was prepared by merely stirring and its photocatalytic behaviour is compared with neat TiO_2 and 20-MWNT-TiO_2 composite catalyst (Figs. 3 and 4). As expected, the irradiated mechanical mixture shows less synergetic effect than the composite catalyst with the same MWNT content. It presents a synergy factor of 1.8 (Table 2) and completely eliminates phenol from the solution within 8 h.

The synergetic effect of MWNT on the activity of the composite catalysts can be explained in terms of its action as adsorbent, dispersing agent and photosensitizer, respectively.

Analysis of Table 2 shows that all the materials have a similar behaviour concerning phenol adsorption during the 60 min dark period, which is indicative of the identical adsorption capacities for different solids. This result is different from the adsorption behaviour in a TiO_2 and activated carbon mechanical mixture [12], where more than 60% phenol in the solution was adsorbed after 1h dark adsorption period for the mixture while less than 10% for neat TiO_2, and the synergetic effect was ascribed to an adsorption of phenol on AC followed by a transfer to titania. With respect to the MWNT-TiO_2 composite catalysts in the present work, the phenol concentration only decreases about 10% for all the solids after dark adsorption. The introduction of MWNT into the composite catalysts does not provide an apparently additive effect on their adsorption capacities. Therefore, the synergetic effect induced by MWNT can favor not only higher rate constants but also higher reaction rates for MWNT-TiO_2 composite catalysts, which may not be merely due to MWNT acting as adsorbent.

On the other hand, the role of MWNT as a dispersing agent is not likely to be a major factor accounting for the observed synergetic effect, since neat TiO_2 shows relatively poor photo-efficiency under visible light irradiation.

Consequently, it is more reasonable to ascribe this synergetic effect to MWNT acting as photosensitizer (Scheme 1) rather than as adsorbent or dispersing agent in the composite catalysts. Considering the semiconductive properties of carbon nanotubes, MWNT may absorb the irradiation and transfer the photo-induced electron (e^-) into the conduction band of the TiO_2 particles (Eq. (1)). This electron transfer between carbon materials and TiO_2 semiconductor or the enhanced photocurrent of the composite materials was also experimentally observed in some other systems [24,36–38]. Simultaneously, a positive charged hole (h^+) might be formed by electron migrating from TiO_2 valence band to MWNT (Eq. (3)). With this understanding, the role played by MWNT can be illustrated by injecting electrons into TiO_2 conduction band under visible light irradiation and triggering the formation of very reactive radicals superoxide radical ion $O_2^{\bullet -}$ (Eq. (2)) and hydroxyl radical $HO^\bullet$ (Eq. (4)), which are responsible for the degradation of the organic compound.

$$\text{MWNT/TiO}_2 \xrightarrow{h\nu} \text{MWNT}^+/\text{TiO}_2^- \quad (1)$$

$$\text{MWNT}^+/\text{TiO}_2^- + (\text{O}_2)_{\text{ads}} \rightarrow \text{MWNT}^+/\text{TiO}_2 + \text{O}_2^{\bullet -} \quad (2)$$

$$\text{MWNT}^+/\text{TiO}_2 \rightarrow \text{MWNT/TiO}_2^+ \quad (3)$$

$$\text{MWNT/TiO}_2^+ + (\text{H}_2\text{O} \rightleftarrows \text{H}^+ + \text{OH}^-)_{\text{ads}} \rightarrow \text{MWNT/TiO}_2 + \text{H}^+ + \text{HO}^\bullet \quad (4)$$

Furthermore, the composite catalyst prepared by the sol–gel method demonstrates higher photocatalytic activity

than the mechanical mixture with the same MWNT content, which suggests that not only the presence of MWNT but also how MWNT and TiO_2 combined should be taken into account to explain the synergetic effect. MWNT embedding in TiO_2 matrix in the composite catalyst can result in an intimate contact, which implies a stronger interphase interaction may be triggered between MWNT and TiO_2 phases in the composite catalyst than in the mixture.

4. Conclusion

MWNT-TiO_2 composite catalysts have been prepared by a modified sol–gel method.

Material characterization indicates a more homogeneous MWNT dispersion in TiO_2 matrix and less agglomeration of TiO_2 particles on MWNT surface, suggesting a strong interphase structure effect between MWNT and TiO_2, so as to increase the surface area of the composite catalysts.

A synergetic effect is observed for the MWNT-TiO_2 composite catalysts on the photocatalytic degradation of phenol under visible light irradiation. This effect was explained in terms of MWNT acting as photosensitizer rather than adsorbent or dispersing agent.

The increase of MWNT/TiO_2 ratio from 5 to 20% favors the enhancement of the synergetic effect on phenol disappearance, which could be correlated to the UV–vis spectra changes of the solids.

Higher photocatalytic activity is observed in case of the composite catalyst prepared by the sol–gel method in comparison to a MWNT and TiO_2 mechanical mixture with the same MWNT content.

The results here presented pointed out the existence of an intimate contact between MWNT and TiO_2 phases in the composite catalysts, able to develop unique electron transfer properties on the resulting materials.

Acknowledgements

This work was supported by Fundação para a Ciência e a Tecnologia, POCTI and FEDER (projects SFRH/BPD/11598/2002 and POCTI/1181/2003) and by CRUP (F-12/03). Thanks to Conférence des Présidents d'Université for financial support "Action intégrée Luso-Française".

Appendix A. Supplementary data

Supplementary data associated with this article can be found, in the online version, at doi:10.1016/j.molcata.2005.02.027.

References

[1] A. Mills, S.L. Hunte, J. Photochem. Photobiol. A 108 (1997) 1.
[2] A. Fujishima, T.N. Rao, D.A. Tryk, J. Photochem. Photobiol. C 1 (2000) 1.
[3] O. Legrini, E. Oliveros, A.M. Braun, Chem. Rev. 93 (1993) 671.
[4] Z. Zhang, C.-C. Wang, R. Zakaria, J.Y. Ying, J. Phys. Chem. B 102 (1998) 10871.
[5] K.Y. Jung, S.B. Park, S.-K. Ihm, Appl. Catal. A 224 (2002) 229.
[6] P.S. Awati, S.V. Awate, P.P. Shah, V. Ramaswamy, Catal. Commun. 4 (2003) 393.
[7] H. Liu, W. Yang, Y. Ma, X. Ye, J. Yao, New J. Chem. 27 (2003) 529.
[8] A. Piscopo, D. Robert, J.V. Weber, J. Photochem. Photobiol. A 139 (2001) 253.
[9] Y.K. Du, J. Rabani, J. Phys. Chem. B 107 (2003) 11970.
[10] K. Nagaveni, M.S. Hegde, N. Ravishankar, G.N. Subbanna, G. Madrao, Langmuir 20 (2004) 2900.
[11] H. Kominami, S. Murakami, J. Kato, Y. Kera, B. Ohtani, J. Phys. Chem. B 106 (2002) 10501.
[12] J. Matos, J. Laine, J.-M. Herrmann, Appl. Catal. B 18 (1998) 281.
[13] C.G. Silva, J.L. Faria, J. Photochem. Photobiol. A 155 (2003) 133.
[14] J. Arana, J.M. Dona-Rodriguez, E.T. Rendon, C.G.I. Cabo, O. Gonzalez-Diaz, J.A. Herrera-Melian, J. Perez-Pena, G. Colon, J.A. Navio, Appl. Catal. B 44 (2003) 153.
[15] A. Di Paola, G. Marci, L. Palmisano, M. Schiavello, K. Uosaki, S. Ikeda, B. Ohtani, J. Phys. Chem. B 106 (2002) 637.
[16] Y.B. Xie, C.W. Yuan, Appl. Catal. B 46 (2003) 251.
[17] Y.B. Xie, C.W. Yuan, Appl. Surf. Sci. 221 (2004) 17.
[18] D. Chatterjee, A. Mahata, Catal. Commun. 2 (2001) 1.
[19] D. Chatterjee, A. Mahata, Appl. Catal. B 33 (2001) 119.
[20] D. Chatterjee, A. Mahata, J. Photochem. Photobiol. A 153 (2002) 199.
[21] J. Moon, C.Y. Yun, K.W. Chung, M.S. Kang, J. Yi, Catal. Today 87 (2003) 77.
[22] V. Iliev, J. Photochem. Photobiol. A 151 (2002) 195.
[23] H. Kisch, L. Zang, C. Lange, W.F. Maier, C. Antonius, D. Meissner, Angew. Chem., Int. Ed. 37 (1998) 3034.
[24] C. Lettmann, K. Hildenbrand, H. Kisch, W. Macyk, W.F. Maier, Appl. Catal. B 32 (2001) 215.
[25] S. Sakthivel, H. Kisch, Angew. Chem., Int. Ed. 42 (2003) 4908.
[26] P. Serp, M. Corrias, P. Kalck, Appl. Catal. A 253 (2003) 337.
[27] M.S. Dresselhaus, in: L.P. Biró, C.A. Bernardo, G.G. Tibbetts, P. Lambin (Eds.), Carbon Filaments and Nanotubes: Common Origins, Differing Applications?, Kulwer Academic Publishers, Dordrecht, 2000, p. 11.
[28] P. Vincent, A. Brioude, C. Journet, S. Rabaste, S.T. Purcell, J.L. Brusq, J.C. Plenet, J. Non-Cryst. Solids 311 (2002) 130.
[29] K. Hernadi, E. Ljubovic, J.W. Seo, L. Forro, Acta Mater. 51 (2003) 1447.
[30] Q. Huang, L. Gao, J. Mater. Chem. 13 (2003) 1517.
[31] A. Jitianu, T. Cacciaguerra, R. Benoit, S. Delpeux, F. Beguin, S. Bonnamy, Carbon 42 (2004) 1147.
[32] J. Sun, L. Gao, Carbon 41 (2003) 1063.
[33] W.D. Wang, P. Serp, P. Kalck, J.L. Faria, Appl. Catal. B 56 (2005) 305–312.
[34] M. Corrias, B. Caussat, A. Ayral, J. Durand, Y. Kihn, P. Kalck, P. Serp, Chem. Eng. Sci. 58 (2003) 4475.
[35] K.S.W. Sing, D.H. Everett, R.A.W. Haul, L. Moscou, R.A. Pierotti, J. Rouquerol, T. Siemieniewska, Pure Appl. Chem. 57 (1985) 603.
[36] P.V. Kamat, I. Bedja, S. Hotchandani, J. Phys. Chem. 98 (1994) 9137.
[37] K.H. Jung, J.S. Hong, R. Vittal, K.J. Kim, Chem. Lett. (2002) 864.
[38] S. Banerjee, S.S. Wong, Nano Lett. 2 (2002) 195.